

Fold-Hopf Bursting in a Model for Calcium Signal Transduction

Lutz Brusch¹, Wolfram Lorenz¹, Michal Or-Guil¹, Markus Bär¹
and Ursula Kummer²

¹ Max Planck Institute for the Physics of Complex Systems,
Nöthnitzer Str. 38, 01187 Dresden, Germany

² Bioinformatics and Computational Biochemistry Group, European Media
Laboratory, Schloss-Wolfsbrunnenweg 33, 69118 Heidelberg, Germany

6. August 2001

Keywords: bursting oscillations, signal transduction, calcium

Abstract:

We study a recent model for calcium signal transduction. This model displays spiking, bursting and chaotic oscillations in accordance with experimental results. We calculate bifurcation diagrams and study the bursting behaviour in detail. This behaviour is classified according to the dynamics of separated slow and fast subsystems. It is shown to be of the Fold-Hopf type, a type which was previously only described in the context of neuronal systems, but not in the context of signal transduction in the cell.

1 Introduction

Nonlinear dynamics has attracted much attention in several scientific fields, predominantly in physics. However, oscillations and chaos have also been discovered within several levels of abstraction in biology and (bio)chemistry. These levels range from populations of organisms (predator and prey systems) [1], individual organisms (circadian and ultradian clocks) [2] down to biochemical reaction pathways (glycolysis) [3] and even individual (bio)chemical reactions (e.g. PO reaction) [4]. In most of these cases, chaotic oscillations have been observed in addition to periodic behaviour. However, the route to chaos can be only studied in experimentally well tractable systems.

In addition to simple periodic and chaotic oscillations, complex periodic

and quasiperiodic oscillations have been observed. Among the complex oscillations, bursting behaviour has been studied thoroughly in the biological context, since it was observed in important processes such as nerve signal conduction [5] and signal transduction [6] within the cell. Several types of bursting have been characterized.

Here, we study a recent model for calcium signal transduction [7]. Calcium ions play a central role as second messengers within the cell. Following the stimulation of agonist receptors at the cell membrane, a cascade of events is triggered which finally leads to the massive liberation of calcium from intracellular stores. Calcium in turn influences multiple processes like gene expression, diverse enzymatic reactions, vesicular transport and embryogenesis [8, 9].

In agreement with experimental results, the model displays simple periodic (spiking), bursting and chaotic oscillations. We compare the bursting behaviour of the complete model to an independent dynamics of its slow and fast subsystems. We study the bifurcation behaviour of the model with one slow variable being used as the bifurcation parameter, considering all other variables to be slaved. This allows the classification of bursting, an approach first used by J. Rinzel [10] for bursting electrical activity in models of nerve cells. We classify the bursting behaviour found in the model under investigation to be of the Fold-Hopf type according to the comprehensive scheme proposed in [11]. So far, this type of bursting had been described in the context of neural activity. Here, we report the first observation in a model for calcium signal transduction. Reasons for this behaviour in terms of the connectivity of the system are discussed.

2 Models for Calcium Dynamics

Many calcium signal transduction models have been developed (for a review see [12]). The one studied here and illustrated in Fig. 1 describes the following scenario: Upon binding of the agonist, the G_α -subunit of the receptor coupled G-protein is activated. Variable a denotes the concentration of activated G_α -subunit. This in turn activates phospholipase C. The concentration of the activated form PLC* is denoted by b . The activated G_α -subunit and PLC* cause the liberation of calcium from the endoplasmic reticulum (ER) and from the extracellular space. The calcium concentrations in the cytosol and in the endoplasmic reticulum are described by the variables c and d . Calcium is pumped back to the ER and to the extracellular space. Moreover, different mechanisms lead to the inactivation of a and b over time.

Variables b and c exhibit negative feedback on variable a by acceleration of the inactivation processes. In addition, variables a and c show autocatalytic behaviour [7]. The autocatalysis in c is an integral compound of a term that

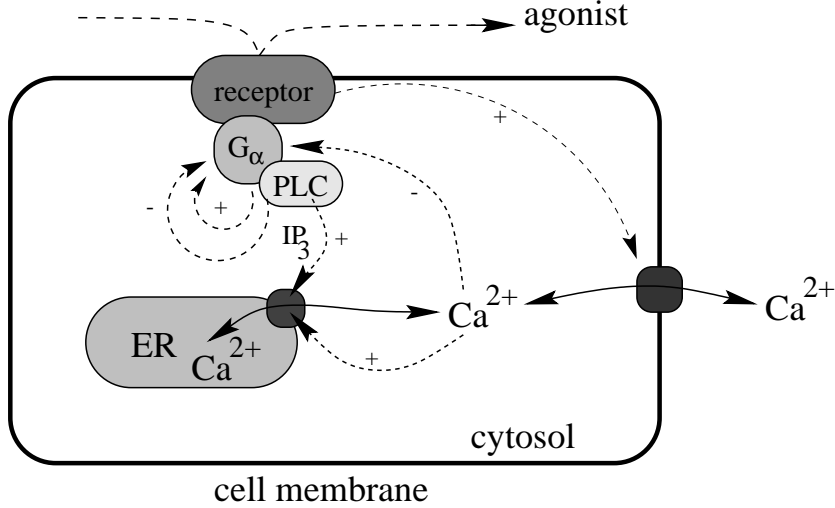


Figure 1: Schematic drawing of the cell with a membrane bound receptor (top) and the endoplasmic reticulum (ER). Dotted arrows denote the modelled influences on the Ca^{2+} fluxes (solid arrows).

describes the activity of a calcium channel at the endoplasmic reticulum (ER). We modified this term compared to the original model in order to make it more realistic. The change mainly ensures the reversibility of calcium diffusion through the channel. The qualitative dynamics of the model is not affected by this change.

The model thus has the following form:

$$\frac{da}{dt} = k_1 + k_2a - \frac{k_3ab}{a + k_4} - \frac{k_5ac}{a + k_6} \quad (1)$$

$$\frac{db}{dt} = k_7a - \frac{k_8b}{b + k_9} \quad (2)$$

$$\frac{dc}{dt} = \frac{k_{10}cb^4(d - c)}{b^4 + k_{11}^4} + k_{12}b + k_{13}a - \frac{k_{14}c}{c + k_{15}} - \frac{k_{16}c}{c + k_{17}} \quad (3)$$

$$\frac{dd}{dt} = -\frac{k_{10}cb^4(d - c)}{b^4 + k_{11}^4} + \frac{k_{16}c}{c + k_{17}} \quad (4)$$

This model exhibits spiking and bursting, as well as chaotic oscillations in dependence on agonist stimulation that is proportional to the parameter k_2 [7]. Moreover, it can be reduced to a 3 variable model which still captures the essential dynamics of the 4 variable model. This reduced model has the following form:

$$\frac{da}{dt} = k_1 + k_2a - \frac{k_3ab}{a + k_4} - \frac{k_5ac}{a + k_6} \quad (5)$$

$$\frac{db}{dt} = k_7 a - \frac{k_8 b}{b + k_9} \quad (6)$$

$$\frac{dc}{dt} = k_{13} a - \frac{k_{14} c}{c + k_{15}} \quad (7)$$

Again, variables b and c exhibit negative feedback on a . The autocatalysis in a is still present. However, the autocatalysis in c is not necessary.

3 Methods

In order to perform a bifurcation and linear stability analysis, the numerical continuation software AUTO97 [13] is employed. AUTO97 computes fixed points and limit cycles of sets of ordinary differential equations. It calculates branches of these solutions under parameter variation, detects bifurcation points and allows to switch to a new branch emerging at a bifurcation. It also monitors eigenvalues respectively Floquet multipliers of the solutions to obtain their linear stability. This method is used for both the analysis of the complete system as well as for its separated slow and fast subsystems.

The classification of the bursting behaviour is carried out according to the following procedure: The bursting behaviour consists of two consecutive phases, a silent phase with slow changes of the variables and an active phase with rapid oscillations of some of the variables whereas others remain slowly varying. Hence, during the active phase, the individual variables change on different time scales and may be grouped into a slow and a fast subsystem, respectively [10]. The encountered bifurcations of the fast subsystem that initiate and terminate the active phase classify the type of bursting according to [11].

4 Results

First, we will focus on the 3 variable model (5)-(7) and later compare its bifurcation structure to the 4 variable model. We choose k_2 as the bifurcation parameter. It denotes the strength of agonist stimulation of the receptor and it is experimentally well studied. All other parameters are kept fixed. The bifurcation diagrams in Fig. 2 show the maximum and minimum of $c(t)$ versus the parameter k_2 .

At $k_2 < 1.3$, the steady state is stable and c increases monotonically with the stimulation k_2 . At $k_2 = 1.3$, a supercritical Hopf bifurcation renders the steady state unstable and stable periodic oscillations coexist with the unstable steady state for $k_2 > 1.3$. As k_2 is increased in the interval $1.3 < k_2 < 2.92$ the oscillations become increasingly complex and develop secondary maxima in $c(t)$. In Fig. 3 examples of spiking (a)-(c) at $k_2 = 2.0$ and bursting (d)-(f) behaviour at $k_2 = 2.9$ are compared.

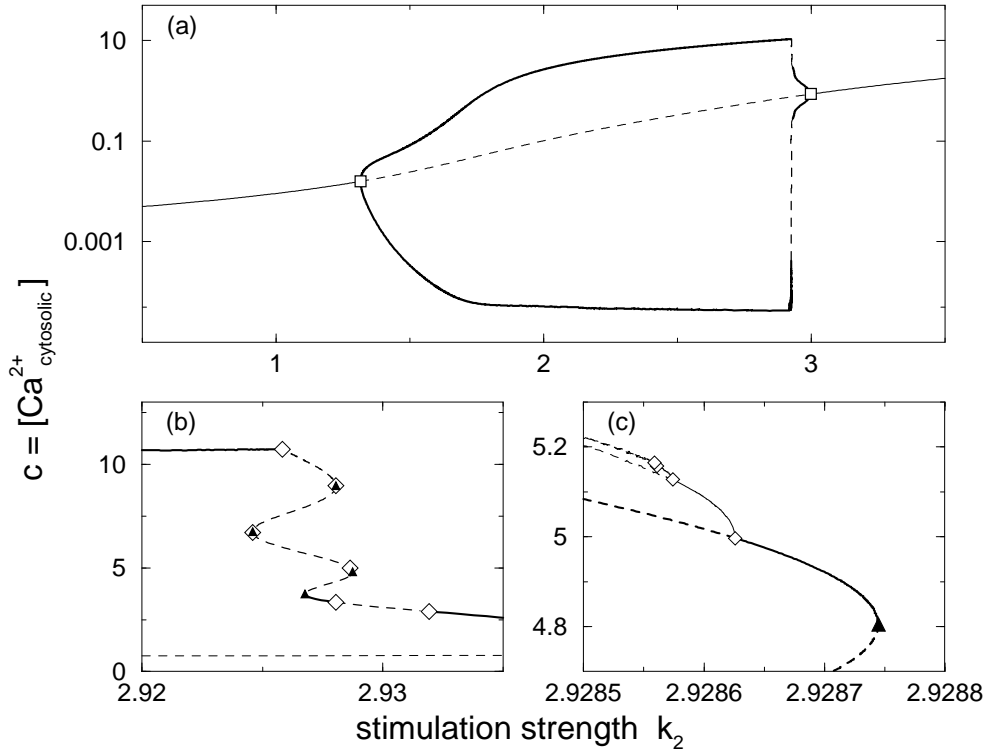


Figure 2: Bifurcation diagrams of complex calcium oscillations (thick curves show maximum and minimum $c(t)$) and steady state behaviour (thin curves in (a,b)) in Eqs. (5)-(7) as function of the agonist level k_2 . Solid (dashed) curves give stable (unstable) solutions. Symbols denote Hopf (open square), saddle-node of periodic orbits (filled triangle) and period doubling (open diamond) bifurcations. (a) covers the whole parameter range of interest whereas (b) is a close-up of the steady state (thin) and the maximum c (thick curve) in the parameter range where periodic bursting is unstable and chaotic behaviour has been observed, e.g. at $k_2 = 2.9259$ in Fig.7 of [7]. (c) shows one of the period doubling cascades with branches of 1 (thick), 2, 4 and 8 irregular bursts (thin) per period. See the text for details. Parameters $k_1 = 0.212$, $k_3 = 1.52$, $k_4 = 0.19$, $k_5 = 4.88$, $k_6 = 1.18$, $k_7 = 1.24$, $k_8 = 32.24$, $k_9 = 29.09$, $k_{13} = 13.58$, $k_{14} = 153$, $k_{15} = 0.16$ are the same as in Fig.7 of [7].

At $k_2 = 2.9258$, the branch of stable bursting undergoes a period doubling bifurcation and turns unstable. Stable oscillations are recovered after a sequence of saddle-node and period doubling bifurcations of periodic orbits as shown in Fig. 2(b). Each hysteresis reduces the number of secondary spikes per burst by one. The intervals of increasing maximum of $c(t)$ with k_2 are unstable due to the saddle-node bifurcations. Those of decreasing maximum are destabilized by pairs of period doubling cascades that occur very close to the saddle-node bifurcations (compare panels (b) and (c) in Fig. 2).

Fig. 2(c) gives a close-up of a period doubling cascade from Fig. 2(b) that is the reason for chaotic behaviour within the parameter intervals between pairs of such cascades. We only show 4 period doubling bifurcations with branches of 1 (thick), 2, 4 and 8 bursts per period. Due to increasing computational effort, the emerging branch with 16 irregular bursts per period is not computed further. This chaotic behaviour has been reported earlier at $k_2 = 2.9259$ (Fig.7 in [7]).

After the periodic oscillations changed back to simple spiking they terminate in the second supercritical Hopf bifurcation at $k_2 = 3.0$. For $k_2 > 3.0$, the steady state is stable and corresponds to over-stimulation with constant high calcium concentration in the cytosol. At large k_2 , the model displays a third Hopf bifurcation where again stable periodic oscillations emerge. However, this feature lies outside the parameter range of interest.

From Fig. 3(d)-(f) it is evident that the smooth oscillations of $b(t)$ evolve on a slower time scale than the secondary spikes of $a(t)$ and $c(t)$. The same solution is given by the dotted curve (with circles) in Fig. 4. Here, the dynamics in the three-dimensional phase space (a, b, c) is displayed by projection onto the (b, a) and (b, c) planes.

In the following, the slow subsystem Eq. (6) and the fast subsystem Eqs. (5),(7) are studied separately. Setting Eq. (6) equal to zero one derives the nullcline

$$a_0(b) = \frac{k_8/k_7 b}{b + k_9} \quad (8)$$

where $db/dt > 0$ for $a > a_0(b)$ and $db/dt < 0$ for $a < a_0(b)$ as follows from the first term on the right hand side of Eq. (6).

The bifurcation diagrams of the fast subsystem Eqs. (5),(7) with b as bifurcation parameter are superimposed in Fig. 4. As b is varied, the steady state solution (thin curves) for a and c shows a hysteresis limited by two saddle-node bifurcations (filled triangles). The lower branch is stable and the middle branch unstable. On the upper branch, a Hopf bifurcation (open square) gives raise to fast oscillations. In the present model, the time scale separation is finite and the solution of the full system (5)-(7) slightly deviates from the curves derived from the fast subsystem.

We gain a qualitative understanding of the complex structure of bursting behaviour if we follow the circles in clockwise direction (arrow) as time

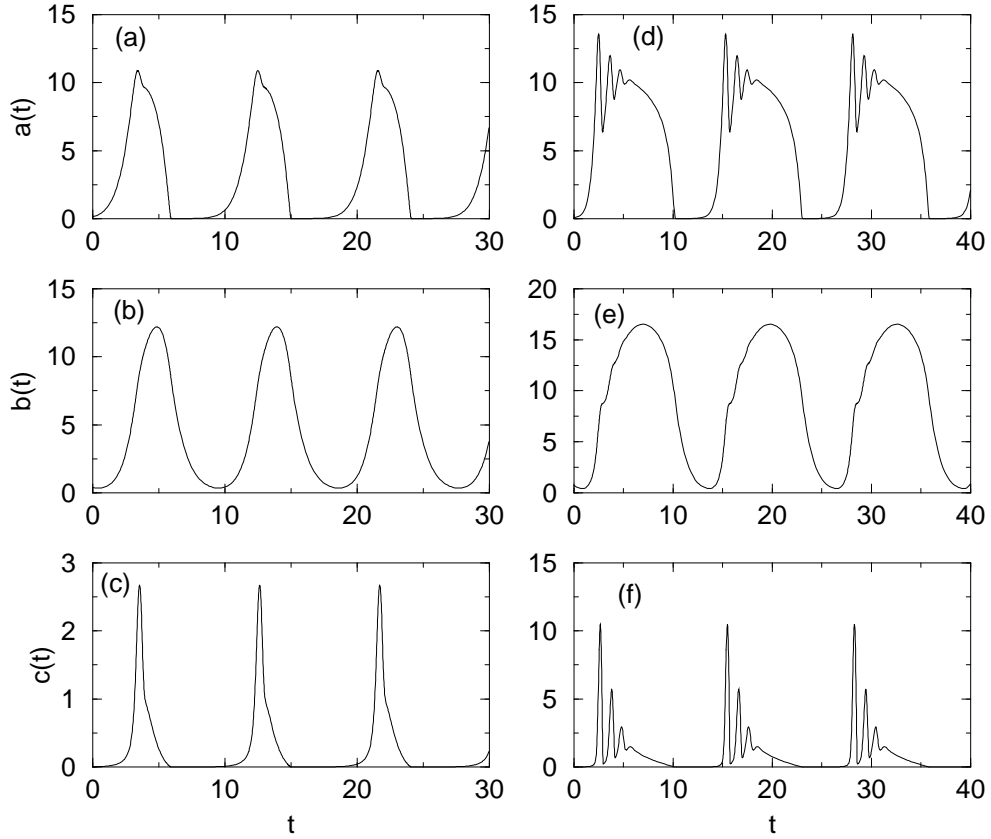


Figure 3: Examples of spiking (a)-(c) at $k_2 = 2.0$ and bursting (d)-(f) at $k_2 = 2.9$ in Eqs (5)-(7). The ordinate labels apply to both panels in each row. The bursts (d)-(f) consist of a silent phase with low values of $a(t)$ and $c(t)$ while $b(t)$ decreases and an active phase with rapid oscillations of $a(t)$ and $c(t)$ when $b(t)$ monotonously increases. The dynamics of $a(t)$ and $c(t)$ occur on a fast and the dynamics of $b(t)$ on a slow time scale. Parameters are the same as in Fig. 2.

progresses. Starting in the silent phase of the burst where a and c are low (compare Fig. 3(d)-(f)) the dynamics are close to the lower stable branch of $a(b)$ and $c(b)$. $db/dt < 0$ holds, since the nullcline (thick dashed curve) lies above. Hence, b will slowly decrease and a and c will adiabatically follow the lower branch in Fig. 4 until the lower saddle-node bifurcation is exceeded. Then, no stable steady state exists any more and the dynamics approach the fast oscillation (thick curve) at larger values of a and c . Now $a > a_0$ and b increases.

The crossing of the saddle-node bifurcation triggers the active phase of the burst which starts with a large spike in $a(t), c(t)$ followed by secondary spikes of decreasing amplitude. The spikes correspond to the branch of fast oscillations in Fig. 4. At larger b these oscillations become smaller and continuously vanish in the supercritical Hopf bifurcation. However, since the time scale separation is finite, the complete dynamics passes the Hopf bifurcation and returns via damped oscillations to the stable focus on the upper branch. This feature has been analysed in detail in a model of enzyme kinetics that shows the same type of bursting [14]. After a short plateau (upper stable steady state) the saddle-node bifurcation at large b is exceeded. The lower steady state is approached and b starts to decrease. This completes one period of the burst.

Since the active phase starts at a saddle-node bifurcation (fold) and ends on a branch of stable foci provided by a supercritical Hopf bifurcation, the present dynamics is an example of Fold-Hopf bursting following the classification by E. M. Izhikevich [11].

We have studied the 4 variable model (1)-(4) in the same way as the 3 variable model (5)-(7). The two models qualitatively show the same behaviour. In Fig. 5 we show the bifurcation diagram of the 4 variable model. The solutions have a similar shape and the bifurcation diagrams of the fast subsystems are qualitatively the same. In the two models $b(t)$ is the only slow variable and the remaining variables constitute the fast subsystem. The type of bursting is the same in the two models.

5 Discussion

We studied the bifurcation and bursting behaviour of a recently proposed model for calcium signal transduction and classified the bursting behaviour to be of Fold-Hopf type. This Fold-Hopf type of bursting has also been observed in the electrical activity of pyramidal cells of the cat hippocampus [15] and in models of the bursting electrical activity in pancreatic β -cells [16]. The authors of the latter paper call it ‘‘tapered’’ bursting. The models have been reduced to the Liénard form which has been studied intensively [17, 18]. The same type of bursting was reported and called ‘‘Type V’’ [17]. However, the

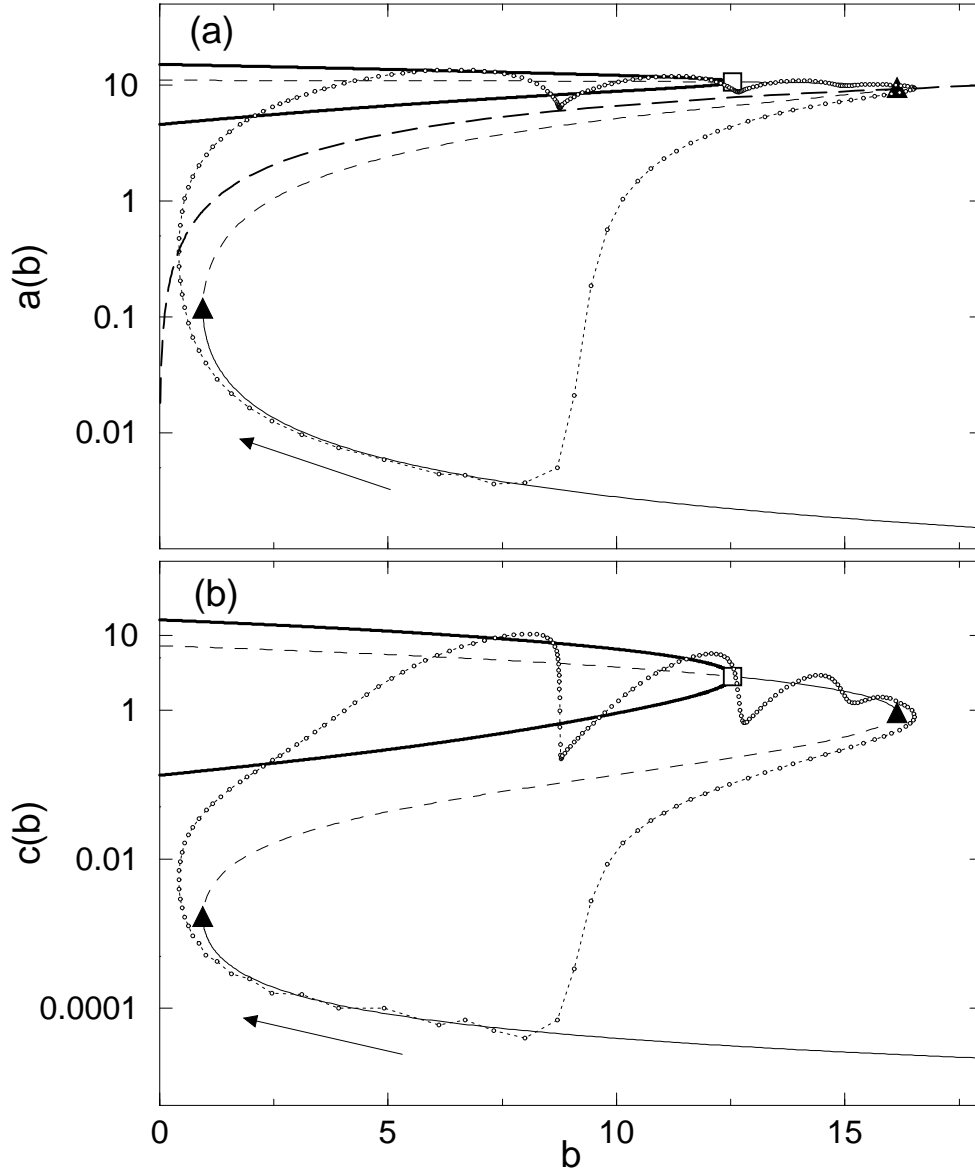


Figure 4: Solutions of the fast subsystem $(a(t, b), c(t, b))$ at $k_2 = 2.9$ as in Fig. 3(d)-(f), projected onto the (b, a) and the (b, c) plane. Thin (thick) curves stand for steady states (maxima and minima of fast oscillations) and dashed (full) curves indicate unstable (stable) solutions. The dotted curve (with circles) represents the projection of the solution of the full system (5)-(7) which is parametrized by time in the clockwise direction following the arrow. Small irregularities at low a and b reflect the finite numerical accuracy. The thick dashed curve in (a) represents the nullcline $b_t = 0$ of the slow dynamics. $b(t)$ increases (decreases) above (below) this curve. Parameters are the same as in Fig. 2.

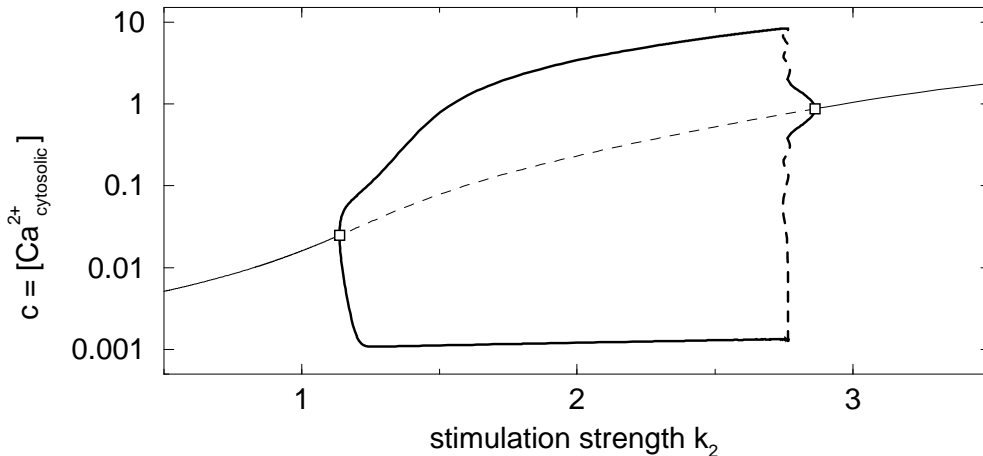


Figure 5: The bifurcation diagram of the 4 variable model (1)-(4) is very similar to that of the 3 variable model (5)-(7). The branch of unstable oscillations (thick dashed) has the same structure as in Fig. 2 . Curves have the same interpretation as in Fig. 2 and parameters are $k_1 = 0.09, k_3 = 0.64, k_4 = 0.19, k_5 = 4.88, k_6 = 1.18, k_7 = 2.08, k_8 = 32.24, k_9 = 29.09, k_{10} = 5.0, k_{11} = 2.67, k_{12} = 0.7, k_{13} = 13.58, k_{14} = 153, k_{15} = 0.16, k_{16} = 4.85, k_{17} = 0.05$.

classification scheme for bursting by E. M. Izhikevich [11] follows a bottom-up approach and provides a systematic nomenclature. It is therefore preferred by us.

In the purely biochemical context, the only previous example for Fold-Hopf type bursting is an abstract enzymatic system [19]. This system is also subject of the study mentioned above [14]. It can be described by three variables and has the following form:

$$\alpha' = \kappa - \delta\phi(\alpha, \beta) \quad (9)$$

$$\beta' = q_1\delta\phi(\alpha, \beta) - \delta\nu(\beta, \gamma) \quad (10)$$

$$\gamma' = q_2\delta\nu(\beta, \gamma) - k_s\gamma \quad (11)$$

It is interesting to compare the topology of this abstract biochemical system with the topology of the calcium signal transduction system studied here. The abstract system involves two negative feedback loops of variable β on α as well as γ on β . It also contains two autocatalysis of the variables γ and β .

The 4 variable model studied here also contains two negative feedback loops as well as two autocatalytic species. However, the 3 variable model which displays the same dynamics contains only one autocatalytic species.

Therefore, the overall topology of the two systems is similar but not the same.

In [20], the model (9)-(11) has been extended by two quickly relaxing variables that account for the finite time scale of allosteric transitions in the enzymatic system. The bursting behaviour was shown to depend on the chosen separation of time scales with the original dynamics (9)-(11) being conserved in the limit of fast allosteric transitions. Our 3 variable and 4 variable models also assume fast allosteric transitions and so far other experimental indications are not available. On the other hand, our models possess a different topology and the results for slow allosteric transitions [20] do not immediately apply to the present situation.

In general, negative feedback loops and simple autocatalysis are very common in biochemical systems. Cooperative or allosteric behaviour in enzymatic systems can be considered to be an autocatalysis for certain ranges of parameters. This behaviour is involved in metabolic regulation and signal transduction. It offers the possibility to fine tune biochemical systems, but also to display a wealth of different dynamic properties. Since the basic requirements for this behaviour are so abundant in the biochemical network in living cells, it is likely that there are many more examples which have not been discovered yet. Bursting behaviour in biology seems to be an integral part of the information processing machinery.

How information is processed in the cell is still not very well understood. However, it has been studied in some detail in the context of calcium signal transduction. It has been shown that the frequency of calcium oscillations encodes information [21, 22, 23, 24]. Fundamental differences in the topology of the signal transduction pathway also offer the possibility to give rise to fundamentally different dynamical behaviour and encode information in this way [7]. In this context, it is of importance which type of bursting behaviour is displayed. Upon variation of the model parameters the locations of bifurcation points shift along the steady state branches in the fast subsystem. For different types of bursting these quantitative changes may trigger different qualitative changes of the bursting behaviour.

Other models of calcium dynamics have recently been studied that also show bursting behaviour but of Fold-Sub-Hopf hysteresis [25] and Sub-Hopf-Fold-Cycle type [26], respectively. In these models the amplitude of the secondary spikes increases as the end of the active phase is approached. This corresponds to unstable foci in their fast subsystems that are provided by subcritical Hopf bifurcations. With our model, the secondary spikes decrease in amplitude. More detailed experimental studies in the future will reveal which type(s) of bursting are predominant in calcium signal transduction.

Acknowledgements:

UK and MO thank the Klaus Tschira Foundation for funding.

References

- [1] M. J. Begon, L. Harper and C. R. Townsend, Ecology: Individuals, Populations, and Communities, 3rd edition, Blackwell Science Ltd. Cambridge, MA (1996).
- [2] L. N. Edmunds (ed.) Cell Cycle Clocks, Marcel Dekker, New York (1984).
- [3] A. Ghosh and B. Chance, Biochem. Biophys. Res. Commun. **16** (1964) 174.
- [4] L. F. Olsen and H. Degn, Nature **267** (1977) 177.
- [5] X. J. Wang and J. Rinzel, Brain Theory and Neural Networks (M. A. Arbib, ed.), The MIT press, Cambridge, MA (1995).
- [6] C. J. Dixon, N. M. Woods, T. E. Webb and A. K. Green, Biochem. J. **269** (1990) 499.
- [7] U. Kummer, L. F. Olsen, C. J. Dixon, A. K. Green, E. Bornberg-Bauer and G. Baier, Biophys. J. **79** (2000) 1188.
- [8] M. J. Berridge, Nature **361** (1993) 315.
- [9] M. J. Berridge, M. D. Bootman and P. Lipp, Nature **395** (1998) 645.
- [10] J. Rinzel, in Mathematical topics in population biology, morphogenesis, and neurosciences, Eds. E. Teramoto and M. Yamaguti, Springer, Berlin, (1987).
- [11] E. M. Izhikevich, Int. J. Bifurcat. Chaos **10** (2000) 1171.
- [12] J. Sneyd, J. Keizer and M. J. Sanderson, FASEB J. **9** (1995) 1463.
- [13] E. Doedel, A. Champneys, T. Fairgrieve, Y. Kusntsov, *et al.*, AUTO97: *Continuation and bifurcation software for ordinary differential equations* (Concordia University, Montreal, 1997).
- [14] L. Holden and T. Erneux, SIAM J. Appl. Math. **53** (1993) 1045.
- [15] E. R. Kandel and W. A. Spencer, J. Neurophysiol. **24** (1961) 243.
- [16] P. Smolen, D. Terman and J. Rinzel, SIAM J. Appl. Math. **53** (1993) 861.
- [17] G. de Vries, J. Nonlinear Sci. **8** (1998) 281.
- [18] M. Pernarowski, SIAM J. Appl. Math. **54** (1994) 814.

- [19] O. Decroly and A. Goldbeter, *J. Theoret. Biol.* **124** (1987) 219.
- [20] M. Kærn and A. Hunding, *J. Theoret. Biol.* **198** (1999) 269.
- [21] W. Li, J. Llopis, M. Whitney, G. Zlokarnik and R. Y. Tsien, *Nature* **392** (1998) 936.
- [22] R. E. Dolmetsch, K. Xu and R. S. Lewis, *Nature* **392** (1998) 933.
- [23] P. De Koninck and H. Schulman, *Science* **279** (1998) 227.
- [24] E. Oancea and T. Meyer, *Cell* **95** (1998) 307.
- [25] J. A. M. Borghans, G. Dupont and A. Goldbeter, *Biophys. Chem.* **66** (1997) 25.
- [26] T. Haberichter, M. Marhl and R. Heinrich, *Biophys. Chem.* **90** (2001) 17.